Appl. Phys. B 74 [Suppl.], S97–S101 (2002)
DOI: 10.1007/s00340-002-0884-x

Applied Physics B
Lasers and Optics

D. YELIN[1]
D. ORON[1]
E. KORKOTIAN[2]
M. SEGAL[2]
Y. SILBERBERG[1,✉]

Third-harmonic microscopy with a titanium–sapphire laser

[1] Department of Physics of Complex Systems, The Weizmann Institute of Science, Rehovot 76100, Israel
[2] Department of Neural Biology, The Weizmann Institute of Science, Rehovot 76100, Israel

Received: 16 September 2001/
Revised version: 29 October 2001
Published online: 27 June 2002 •

ABSTRACT We demonstrate third-harmonic microscopy of thin biological objects using a Ti:sapphire laser source. A very simple modification to the collection and detection systems of the microscope allows for the detection of the third-harmonic signal near 270 nm. We show that, using a Ti:sapphire laser, we can combine third-harmonic imaging with two-photon excitation fluorescence simultaneously. Compared to other possible laser sources for third-harmonic microscopy, the Ti:sapphire laser provides better optical resolution, better power availability, and is less absorbed in water. We find that the Ti:sapphire laser is the most suitable laser source for third-harmonic microscopy for thin biological specimens.

PACS 42.65.Ky; 87.64.Vv; 42.62.Be

1 Introduction

The field of nonlinear light microscopy has been rapidly developing since the appearance of compact femtosecond lasers. Two-photon [1] and three-photon [2] fluorescence microscopy show better axial resolution and improved signal-to-background ratios compared with standard laser scanning fluorescence microscopy. Second-harmonic generation was also used for microscopy of certain crystal samples [3] and for specialized biological imaging [4]. Third-harmonic generation (THG) microscopy has recently been studied as a probe to characterize transparent specimens [5–9]. In THG microscopy, third-harmonic light is generated at the focal point of a tightly focused short-pulse laser beam. When the medium at the focal point is homogeneous, the third-harmonic waves generated before and after the focal point interfere destructively, resulting in zero net THG [10]. However, when there are inhomogeneities near the focal point, such as an interface between two media, the symmetry along the optical axis is broken and a measurable amount of the third harmonic is generated. Due to its nonlinear nature, the third-harmonic light is generated only in close proximity to the focal point. Therefore, high depth resolution can be obtained, allowing THG microscopy to perform optical sectioning and to construct three-dimensional images of transparent samples. Since all materials have nonvanishing third-order susceptibilities, THG microscopy can be utilized as a general-purpose microscopy technique, with no need for fluorescence labeling or staining. Recently, we have demonstrated the applicability of THG microscopy to biology on scales that vary from the subcellular to millimeter-size organisms [8, 9]. The need for efficient THG in the sample together with low average laser power to avoid heating dictates a laser source that operates with femtosecond pulses. The lasers that are often used for THG microscopy are a synchronously pumped OPO at a wavelength of 1500 nm [5, 11], a low-repetition-rate OPA at 1200 nm [6, 7], and a Cr:Forsterite laser at 1240 nm [12]. Millard et al. studied a compact fiber laser at 1560 nm as a source for third-harmonic microscopy [13]. All these lasers are in the infrared (IR), above 1200 nm; thus, the third-harmonic signals are in the visible range. These visible signals are compatible with the integral collection optics of standard microscope systems. Also, excitation light in the IR undergoes low scattering and therefore has large penetration depth in scattering specimens. On the other hand, absorption in water increases dramatically with the increasing wavelength [14]: absorption that might lead to unwanted heating and power loss. Also, the transmission of standard large numerical aperture (NA) objectives is shown to be low at long wavelengths, adding a loss that may limit the available power that can be delivered from relatively weak laser sources to the sample. In addition, the transverse and axial resolutions degrade with the increasing wavelength, not only because of the theoretical spot size, but also because of optical aberrations of the objectives, which are usually designed for the visible range. In this publication we demonstrate improved THG microscopy by using a Ti:sapphire laser. The Ti:sapphire laser is the most common, compact, and available laser source of femtosecond pulses. It has many configurations for a wide range of intensities, pulse durations, and wavelength tunability near 800 nm. The absorption coefficient of water [14] for this wavelength is $0.02\,\mathrm{cm}^{-1}$, much smaller then for 1240 nm ($1\,\mathrm{cm}^{-1}$) or for 1500 nm ($10.8\,\mathrm{cm}^{-1}$). Ti:sapphire radiation is also transmitted better through most objectives. We measured transmission of a standard large numerical aperture (Zeiss, plan-apochromat NA = 1.4, ×63) for various wavelengths. The transmissions for 810, 1240, and 1500 nm were 62%, 23%, and 20% respectively. These large losses at long wavelengths are probably due to fact that the anti-reflection coatings on the objective glass surfaces were designed for

✉ E-mail: Feyaron@wisemail.weizmann.ac.il

the visible range. We note that, on the other hand, 810-nm light scatters more compared with longer wavelengths [15], and therefore might be less suitable for thick and scattering samples.

The main limitation of the Ti:sapphire laser for THG microscopy is the wavelength of the third harmonic, which is in the ultra-violet (UV) near 270 nm. This THG signal would be completely absorbed in standard microscope slides or even in thin cover slips. Since THG is directional, the microscope setup is in transmission mode, where the laser light arrives through the objective, and the THG signal is collected through the original microscope condenser [8]. In order to detect the UV signals, we have replaced the condenser optics and the deflecting mirror with UV-grade optics. Although the third harmonic is absorbed in water only slightly more than visible light (absorption coefficient of $2.36 \times 10^{-4}\,\mathrm{cm}^{-1}$ for 270 nm [16] and $2 \times 10^{-4}\,\mathrm{cm}^{-1}$ for 500 nm [17]), it is absorbed in large biological molecules and in membranes. This may cause degradation of the signal in some areas in the specimen. This degradation should be taken into consideration when interpreting the THG image of a given specimen. Another possible effect due to the UV third harmonic is possible damage to the biological object. This problem should be addressed in more detailed experiments with live biological objects. Such experiments are beyond the scope of this work; however we believe that the practical effect will be minor due to the very weak intensity of the UV radiation, which is of the order of a few picowatts. Note that some UV radiation is generated through the third-harmonic process even in standard two-photon excitation fluorescence microscopy; hence such damage, if it occurs, could affect both third-harmonic and two-photon microscopy.

2 Experiment

The experimental configuration for a third-harmonic microscope using a Ti:sapphire laser is shown in Fig. 1. As an imaging platform, we used a Zeiss Axiovert-135 microscope, which was modified into a scanning THG microscope. The laser source is a Spectra-Physics Tsunami that provides 100-fs pulses at a wavelength of 810 nm at a repetition rate of 80 MHz. The laser beam is coupled through one of the microscope ports and is focused into the sample by a microscope objective. The focal point is scanned in the x-y plane using two optical scanners, and along the z axis using the motorized stage of the microscope. The original detection scheme is replaced by UV-grade optics: the third-harmonic light at the wavelength of 270 nm is collected by a UV-grade fused-silica condenser ($f = 16$ mm, $D = 21.4$ mm), and measured by a UV-grade photomultiplier tube (PMT, Hamamatsu R4220) after filtering out the fundamental wavelength using a band-pass interference filter (center wavelength 265 nm, FWHM = 25 nm). The current generated by the photomultiplier was amplified using a radio-frequency lock-in amplifier (Stanford Research Systems, model SR844), which uses the synchronization output of the Ti:sapphire oscillator as a reference. This lock-in amplifier allows signal amplification with very good noise rejection at very short integration times (down to 100 μs per pixel) without the need for additional chopping of the signal. The output signal from the lock-in amplifier was fed into a computer, which synchronizes the scanning process and the data collection.

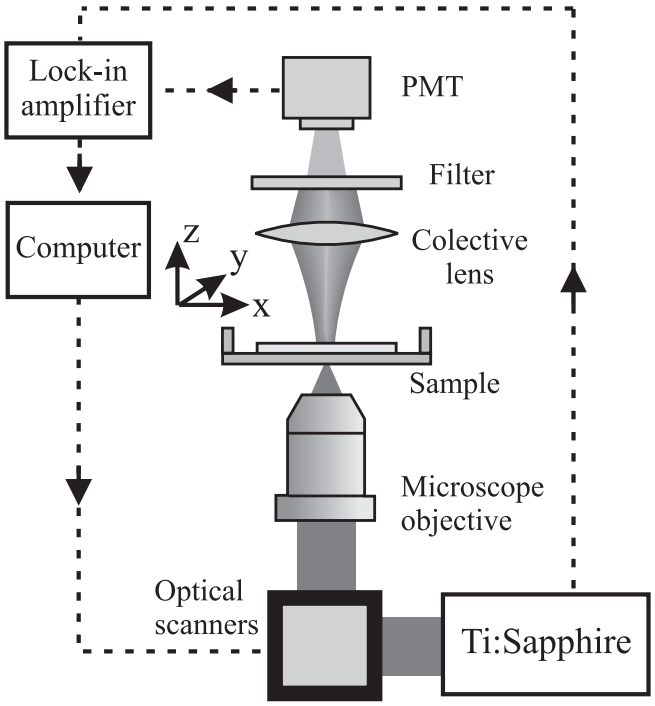

FIGURE 1 Optical setup for third-harmonic microscopy using a Ti:sapphire laser. The optics of the original detection system is replaced with UV-grade optics. The specimen is mounted without cover glass

To demonstrate the performance of the Ti:sapphire laser as a source for THG microscopy we imaged a fixed epithelial cell with three different light sources: the Ti:sapphire laser at 810 nm, a Cr:Forsterite laser at 1240 nm, and the signal beam from an OPO (Spectra Physics – Opal), pumped by the Ti:sapphire laser, at 1500 nm. The specimen was immersed in a buffer solution without cover glass to avoid absorption of the THG signal. The image obtained with the Ti:sapphire laser is shown in Fig. 2a. Images of the same cell at the same field of view using the Cr:Forsterite laser and the OPO are shown in Fig. 2b and c, respectively. All images were obtained using an oil-immersed, NA = 1.4, ×100 objective. While there is no significant difference between the Cr:Forsterite laser and the OPO images, the image using the Ti:sapphire laser appears much clearer and sharper, and reveals more details with better resolution. In addition, the background noise caused by stray light from the surroundings was lower in the UV range, compared to the visible. Therefore, together with the lock-in-amplifier operation, the microscope exhibits very good noise rejection, and measurements can be performed in much less stringent lighting conditions.

In order to compare the depth resolution for the different wavelengths we performed z-scans with the three sources across an interface between glass and air [5]. The results are shown in Fig. 3a and b for Zeiss plan-apochromat NA = 1.4, ×100 and NA = 1.4, ×63 objectives, respectively. Note that the ×100 objective provides much better axial resolution at all three wavelengths, although both objectives have the same numerical apertures. For both objectives the Ti:sapphire

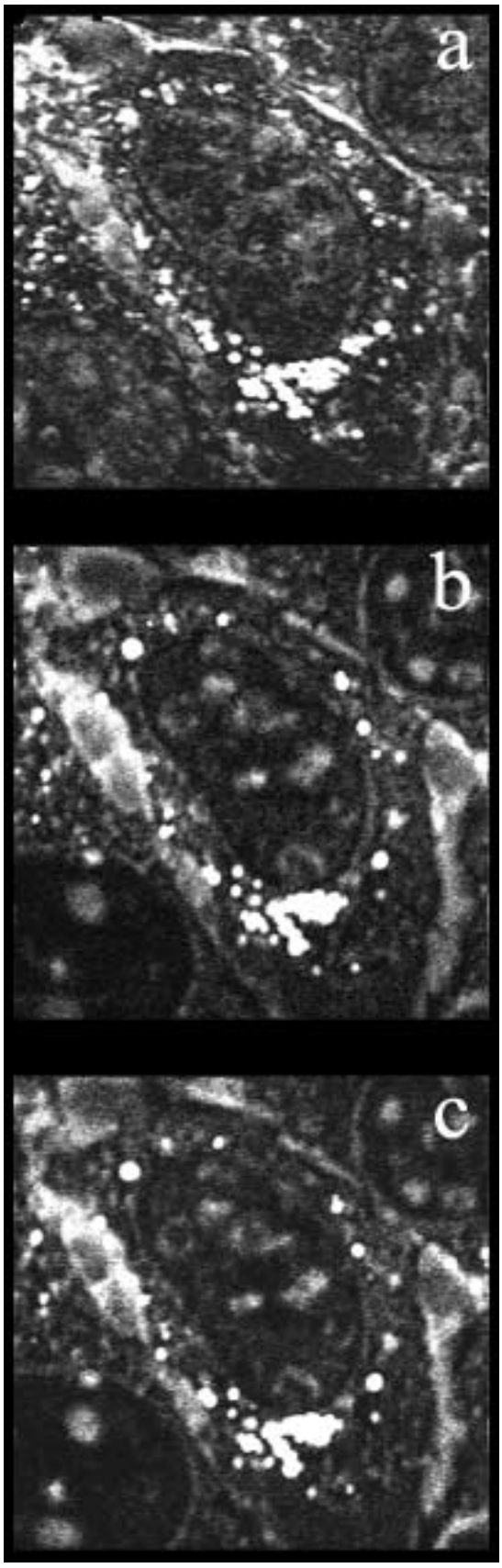

FIGURE 2 Digitized images of a fixed epithelial cell using: **a** Ti:sapphire laser at 810 nm, **b** Cr:Forsterite laser at 1240 nm, **c** an OPO at 1500 nm. The field of view is $20 \times 20\ \mu m^2$. The image using the Ti:sapphire laser appears clearer and sharper, and reveals more details with better resolution

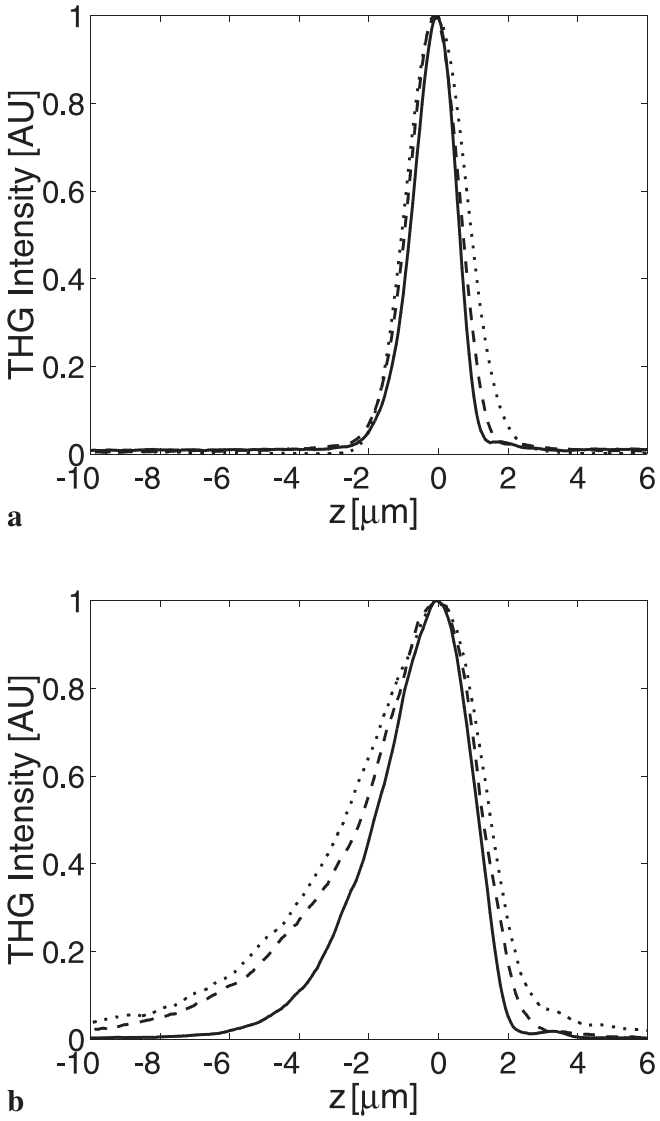

FIGURE 3 **a** z-scans across a glass–air interface using a NA = 1.4, ×100 objective with three light sources: Ti:sapphire laser at 810 nm (*solid line*), Cr:Forsterite laser at 1240 nm (*dashed line*), and the signal beam from an OPO at 1500 nm (*dotted line*). **b** Similar z-scans using a NA = 1.4, ×63 objective. Note the better axial resolution of the Ti:sapphire laser for both objectives

laser (solid line) exhibited better depth resolution (1.35 μm and 3 μm FWHM for the ×100 and ×63 objectives, respectively), compared with the Cr:Forsterite laser (dashed line) and the OPO (dotted line). The axial resolution achieved by the Ti:sapphire laser is only slightly smaller then the calculated focal length of a Gaussian beam (1.22 μm).

Shown in Fig. 4 is a set of THG optical sections of a fixed neuron using the Ti:sapphire laser. The sections are separated by 2 μm, where the top-left section is closer to the glass substrate and the bottom-right section is the top of the cell. By comparing these sections with our previous work with neurons [8], we note that the resolution is improved.

In a previous work [9], we showed that THG microscopy could be utilized for very thick (3-mm) samples for optical tomography of small objects. We found that the Ti:sapphire laser is not suitable for this purpose. The reason for this is

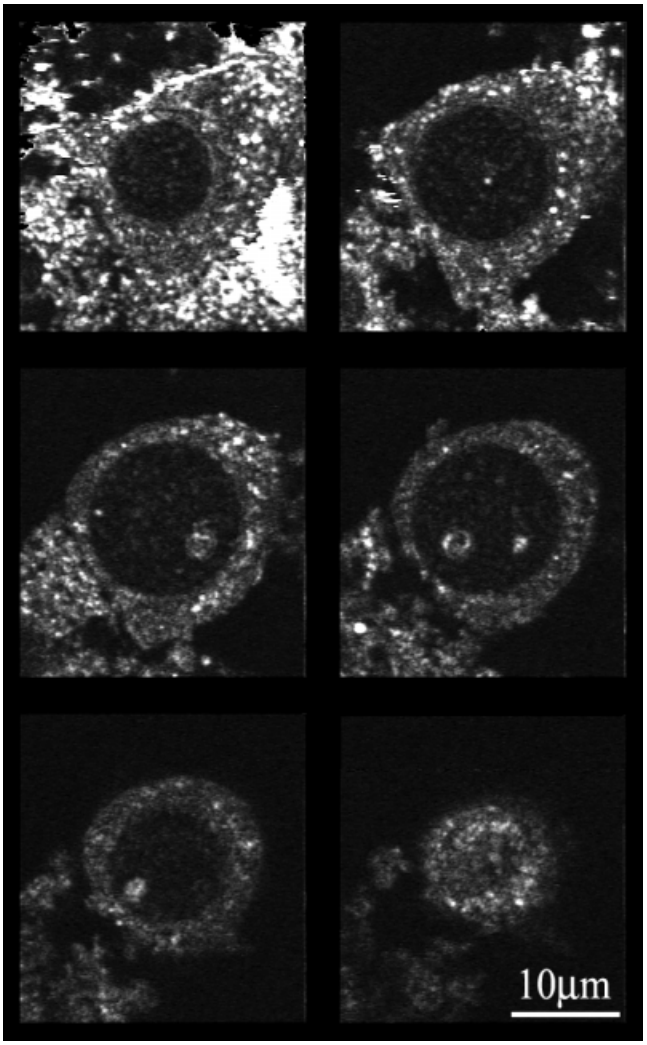

FIGURE 4 Set of THG optical sections of a fixed neuron using the Ti:sapphire laser. The sections are separated by 2 μm, where the *top-left section* is closer to the glass substrate and the *bottom-right section* is the top of the cell. The *dark round region* at the center of the cell is the nucleus. Inside it two bright nucleoli can be observed (cf. [8])

probably the very large scattering cross section for the UV third-harmonic light. Trying to avoid the scattering problem with a clearing solution failed since the UV light is absorbed in the solution.

3 Simultaneous third-harmonic and two-photon excitation fluorescence imaging

Third-harmonic microscopy is a general-purpose technique and provides mainly structural information. It cannot give information on specific molecules or organelles. This problem can be solved by combining third-harmonic imaging with specific fluorescence labeling.

Using a Ti:sapphire laser, it is possible to perform third-harmonic and two-photon excitation fluorescence (TPEF) imaging with a single laser source. Using a single laser source is most desirable for some reasons: first, the problem of chromatic aberration does not exist and therefore the third harmonic and the TPEF are generated exactly at the same depth. Second, the microscope system and its alignment are most simplified using only one laser beam and, by using two separate collection paths, in the forward direction for the THG and in the backward direction for the TPEF, a single scan is sufficient to provide the combined image.

Combined images of THG and TPEF of a fixed neuron are presented in Fig. 5a for $z = 0$ and in Fig. 5b for $z = 4$ μm. The cell nucleus was labeled with DAPI (maximum excitation at 350 nm, maximum emission at 450 nm). The two data channels were combined for false-color images (purple for THG and green for TPEF). In this case, the THG and the TPEF appear quite complementary: the THG signal

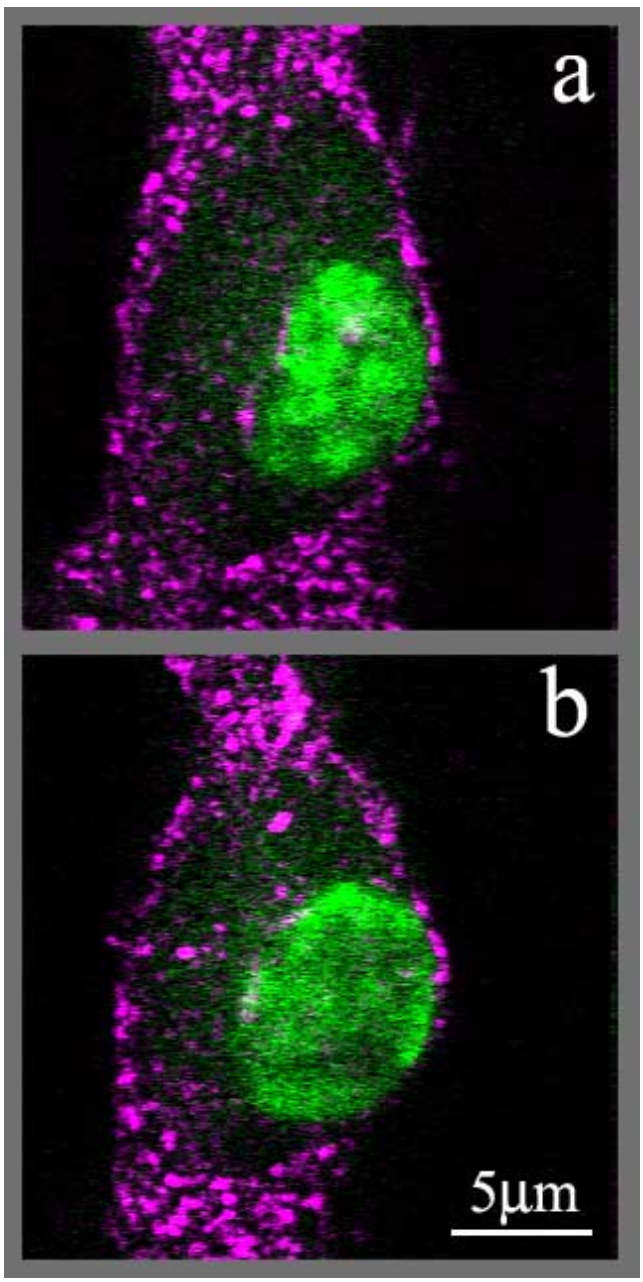

FIGURE 5 Combined images of THG and TPEF of a fixed neuron **a** for $z = 0$ and **b** for $z = 4$ μm. The cell nucleus was labeled with DAPI (maximum excitation at 350 nm, maximum emission at 450 nm). The two data channels were combined for false-color images (purple for THG and green for TPEF)

from the nucleus comes only from the nucleolus (which can be noted in Fig. 5a) and the TPEF from the DAPI is generated mainly at the nucleus. The nucleolus cannot be resolved by the TPEF image only. The THG image is shown here to provide the general shape of the cell as a frame of reference in which specific fluorescence labeling is used. All this can be done in a single scan of a single laser beam. Ti:sapphire lasers are already used in commercial TPEF microscopes. Adding the THG imaging capability to these microscopes involves only adding a detection path in the forward direction for the detection of the UV third-harmonic signal.

4 Conclusion

In conclusion, our results show that with a few simple and inexpensive modifications to the collection and detection optics of the microscope, the Ti:sapphire laser is the most straightforward and suitable source for THG microscopy for imaging of thin samples. Since Ti:sapphire lasers are already used in commercial two-photon fluorescence microscopes, such microscopes can be easily adapted to THG microscopy. The combined two-photon and THG microscope could produce simultaneously functional fluorescence images together with detailed structural information from the same optical section.

ACKNOWLEDGEMENTS The authors wish to acknowledge support from the Israel Science Foundation and the German BMBF.

REFERENCES

1 W. Denk, J.H. Stricker, W.W. Webb: Science **248**, 73 (1990)
2 S. Maiti, J.B. Shear, R.M. Williams, W.R. Zipfel, W.W. Webb: Science **275**, 530 (1997)
3 R. Gauderon, P.B. Lukins, C.J.R. Sheppard: Opt. Lett. **23**, 1209 (1998)
4 G. Peleg, A. Lewis, O. Bouevitch, L. Loew, D. Parnas, M. Linial: Bioimaging **4**, 215 (1996)
5 Y. Barad, H. Eizenberg, M. Horowitz, Y. Silberberg: Appl. Phys. Lett. **70**, 922 (1997)
6 M. Muller, J. Squier, K.R. Wilson, G.J. Brakenhoff: J. Microsc. **191**, 266 (1998)
7 J.A. Squier, M. Muller, G.J. Brakenhoff, K.R. Wilson: Opt. Express **3**, 315 (1998)
8 D. Yelin, Y. Silberberg: Opt. Express **5**, 169 (1999)
9 D. Yelin, Y. Silberberg: Microsc. Anal., November, 15 (2000)
10 R. Boyd: *Nonlinear Optics* (Academic, New York 1992)
11 L. Canioni, S. Rivet, L. Sarger, R. Barille, P. Vacher, P. Voisin: Opt. Lett. **26**, 515 (2001)
12 S. Chi-Kuang, C. Shih-Wei, T. Shi-Peng, S. Keller, U.K. Mishra, S.P. Denbaars: Appl. Phys. Lett. **77**, 2331 (2000)
13 A.C. Millard, P.W. Wiseman, D.N. Fittinghoff, K.R. Wilson, J.A. Squier, M. Muller: Appl. Opt. **38**, 7393 (1999)
14 J.A. Curcio, C.C. Petty: J. Opt. Soc. Am. **41**, 302 (1951)
15 H.J. van Staveren, C.J.M. Moes, J. van Marle, S.A. Prahl, J.C. van Gemert: Appl. Opt. **30**, 4507 (1991)
16 T.I. Quickenden, J.A. Irvin: J. Chem. Phys. **72**, 4416 (1980)
17 R.M. Pope, E.S. Fry: Appl. Opt. **36**, 8710 (1997)